Removal of Reactive Dyes from Wastewater using Cyclodextrin Functionalized Polyacrylonitrile Nanofibrous Membranes

Foza Foroozmehr, Sedigheh Borhani, and Seyed Abdolkarim Hosseini

***Abstract*— Electrospinning of nanofibers with cyclodextrin (CD) is attractive because the produced fibers can potentially increase the efficiency of nanofibrous membranes by facilitating the complex formation with organic compounds and high surface area of the nanofibers. In this work, polyacrylonitrile (PAN) nanofibers functionalized with β–cyclodextrin (βCD) during an electrospinning process were used to treat a reactive dye wastewater stream by dynamic method. It was found that the dye removal efficiency was increased from 15.5% for PAN to 24% for PAN/βCD nanofiber mats. The low efficiency of PAN/βCD membranes was due to the decrease in the βCD content during the filteration process because of the high solubility of βCD in aqueous solutions. By crosslinking βCD through a polycondensation process, the PAN nanofibrous membranes containing βCD polymer (βCDP) were prepared and used for filtration. Compared with PAN nanofibers, it was found that the dye removal efficiency improved more than two times by using PAN/βCDP nanofibers. In such circumstances, due to the decrease in the water solubility of βCDP, the βCDP content in nanofibers didn't change during filtration; therefore, the dye removal efficiency of the PAN/βCDP nanofibers was higher than that of the PAN/βCD ones. The XRD results also showed that inclusion complexes between the βCD cavities and dye molecules were formed.**

***Keywords*: β–cyclodextrin, inclusion complex, nanofibrous membrane, reactive dye, wastewater**

I. Introduction

Textile industries consume huge volumes of water and chemicals. The chemicals used in this industry vary from inorganic compounds to polymers and organic products. This makes the composition of the wastewater very complex and potentially toxic [1-4]. Among chemicals in textile wastewater, dyes are considered important pollutants [2]. Although the exact amount of dyes produced in the world is not known, it is estimated that the commercially available dyes are more than 10,000 tons per year [5]. Exact data regarding the quantity of dyes discharged in the environment are also not available.

Among the dyes used for cellulosic fabrics, reactive dyes are the most important ones. The amount of the hydrolysed dye, after the completion of the reactive dyeing process, is more than 800 mg/l. The reactive dyes fixation rate is in the range of 60 – 70 %. This range will be higher when the dyes contain two reactive groups [3]. Thus, more than 40 % of the reactive dyes are discharged in the effluent, resulting in highly colored wastewater. Additionally, reactive dyes, in both ordinary and hydrolyzed forms, are not easily biodegradable and therefore, even after extensive treatments, the color may still remain in the effluent [3].

Reactive dyes cannot be easily removed by conventional wastewater treatment systems since they are stable against light, heat and oxidizing agents and are not biologically degradable. In fact, they are identified as problematic compounds in the textile wastewater [6]. Conventional processes, such as coagulation and flocculation methods adopted for decolorizing effluents containing reactive dyes, are no longer able to achieve adequate dye removal [3]. Adsorption methods have been invariably successful in decolorizing textile effluents, but this application is limited by high cost. Among the wastewater treatment processes, membrane separation can remove dyes from textile wastewater. Ultrafiltration cannot completely decolorize the reactive dye effluent and it does not remove low molecular weight dyes either [7]. Nanofiltration and reverse osmosis can treat effluents with high efficiency. But these processes are not commercially used because of their high cost.

Nanofibrous membranes are the most suitable replacements for common membranes. These membranes have a low basis weight, high permeability, a low pressure drop and a small pore size, which make them appropriate for a wide range of filtration applications. In addition, they have unique properties like high specific surface area; good inter connectivity of pores and the potential to incorporate active chemistry or functionality on a nanoscale. Therefore, nanofibrous membranes have been extensively studied for air and liquid filtration [8,9].

Cyclodextrins (CDs) can be used to functionalize the nanofibers. These cyclo oligosaccharides contain α(1,4)-linked glucopyranoside units having either six, seven, or eight glucose units arranged in a cyclic structure and accordingly, they are named as α-, β- and γ-cyclodextrins, respectively [10]. They have a cavity in their structure whose inner surface is hydrophobic, whereas the exterior surface is hydrophilic. The hydrophobic cavity of CD results in forming non-covalent host– guest complexes with various small molecules and macromolecules [11]. Because the physical and chemical properties of the incorporated guest compounds can be tailored by

F. Foroozmehr, S. Borhani and S. A. Hosseini are with the Department of Textile Engineering, Isfahan University of Technology, Isfahan, Iran. Correspondence should be addressed to S. Borhani (e-mail: sborhani@cc.iut.ac.ir).

complexation with CDs, they are used in a variety of application areas, such as pharmaceuticals, foods, cosmetics, home/personal care products, textiles, etc. The functionalization of nanofibers with cyclodextrins could be extremely interesting since nanowebs containing CDs would have a unique characteristic that could potentially increase the efficiency of nanofiber-based filters by facilitating the complex formation with organic compounds and significantly increasing the surface area of the nanofibers [10,12].

During the last years, there have been few studies on incorporating cyclodextrins in electrospun fibers. For instance, poly(acrylic acid) nanofibers were crosslinked with βCD in order to produce water insoluble polyelectrolyte nanowebs [13]. To detoxify the nerve agents, a catalyst was synthesized from βCD and o-iodosobenzoic acid. This modified βCD was incorporated into polyvinyl chloride (PVC) nanofibers in order to develop functional nanofibrous membranes that could provide protection from chemical warfare stimulants [14]. Poly(methyl methacrylate) (PMMA) nanofibers have been electrospun with phenyl carbomylated and azido phenyl carbomylated βCD to try to capture phenolphthalein as a model of organic molecules for waste treatment [15]. Poly(N-vinylpyrrolidone) composite nanofibers were electrospun with βCD [16]. In another study, nanofibers containing gold nanoparticles were produced and βCD was used as a stabilizing and reducing reagent [17]. Poly(ethylene oxide) (PEO) nanofibers containing cyclodextrin/poly(ethylene glycol) inclusion complexes were produced [18]. Numerous researchers have electrospun PMMA [12], PEO [19] and polystyrene (PS) fibers [20] functionalized with cyclodextrins. CD–menthol inclusion complexes in the electrospun PS and PMMA nanofibers were incorporated to produce functional nanofibers that contained fragrances/flavors with high temperature stability [11,21]. Functionalized polystyrene fibrous membranes showed the potential for efficient removal of organic compounds (e.g.: phenolphthalein) from solutions by formation of inclusion complexes with the βCD molecules [10]. Electrospun PMMA nanowebs containing βCD were produced, proving that they could entrap organic vapors such as aniline, styrene and toluene from the surroundings due to the inclusion complexation with βCD which was present on the fiber surface [22]. A novel βCD/poly(vinyl alcohol) (PVA) nanofibrous membrane with the function of molecular capturing was prepared. It was shown that βCD/PVA could recognize small hydrophobic molecules such as ferrocene (Fc) by forming inclusion complexes [23].

In this work, our aim is to study the ability of β-cyclodextrin functionalized polyacrylonitrile nanofibers to remove reactive dyes from wastewater. To investigate the ability of webs to capture dye molecules, a cross flow filtration system was used to treat the reactive dye wastewater. In order to prevent dissolving of cyclodextrin in water, it was crosslinked with citric acid. The electrospinning process was carried out with different concentrations of β– cyclodextrin polymer (βCDP). Then the dye removal performance of the membranes was analyzed.

II. Experimental

A. Materials

β–Cyclodextrin(βCD) and Polyethylene glycol (PEG) (Mn=400 g/mol) were purchased from Sigma – Aldrich, (USA). Polyacrylonitrile (PAN) powder (Mw=100,000 g/mol) was kindly prepared by Polyacryl Co, Isfahan (Iran).Citric acid monohydrate and N, N-dimethyl formamide (DMF) were purchased from Merck, (Germany) and C.I. Reactive Blue 13 with the chemical structure presented in Fig. 1 was used.

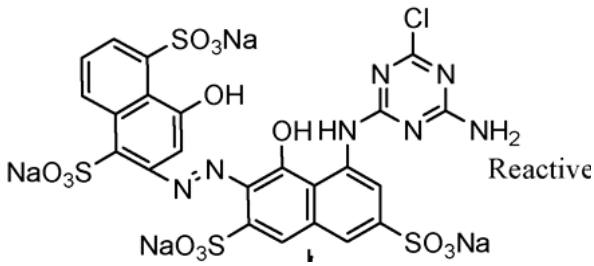

Fig. 1. Chemical structure of C.I. Reactive Blue 13.

B. Electrospinning of Cyclodextrin Functionalized Polyacrylonitile (PAN/βCD)

To prepare the electrospinning solutions, βCD was dissolved in DMF and then PAN was added to the solution and vigorously stirred at the ambient temperature. βCD concentration was 10 and 50 wt% with respect to the PAN concentration. PAN concentration was 13 wt% with respect to the solution. The solution was placed in a 1 ml syringe fitted with a metallic needle with the inner diameter of 0.7 mm. The Electrospinning process was done according to conditions described in Table I. Nanofiber webs were electrospun onto carbon coated polyurethane foam substrates to supply suitable mechanical properties and allow pleating filter production. The substrates were wrapped around a drum rotating at 75 rpm. Meanwhile, the traverse speed of the pump was 4 cm/min. The electrospinning process was carried out in a horizontal position at room temperature.

C. Measurements and Characterization

The viscosity of the polymer solutions was measured at 20°C using a Brookfield DVII + Pro viscometer.

The morphology of fibers was investigated by a Scanning Electron Microscope (Philips SEM, XL-30, Netherlands). The diameter of the fibers was measured from SEM images using measurement software. The diameter of 100 fibers was measured.

The surface of the nanofibers was analyzed by attenuated total reflection fourier transform infrared (ATR-FTIR). Fourier transform infrared (FTIR) spectroscopy studies were performed with a Bomem MB – Series 100 spectrometer (Canada) in the range of 400 to 4000 cm^{-1}. X–Ray diffraction analyses were carried out using a Philips X'Pert system (Netherlands), with CuKα radiation

(λ=1.54 Å) to examine if any βCD crystalline aggregates were present in the PAN nanofibers. Scans were run in the wide angle of 5–50° and the scan speed of 1° /min. Air permeability of nanofiber membranes was measured by a Shirley permeation analyzer (England) at a relative humidity of 65%, an ambient temperature of 25°C, and a pressure drop of 100 Pa.

D. Filtration

A cross-flow filtration system with the active filtration area of 0.04 m^2 was used to test the filtration efficiency of the membranes. The set-up is shown in Fig. 2.

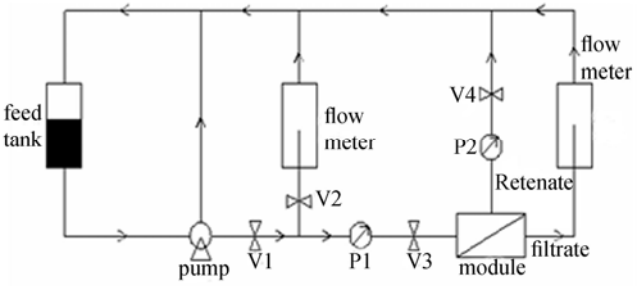

Fig. 2. Schematic of filtration system [24].

The applied pressure was 1.9 bar and the filtration duration was 1 hour at room temperature. The pH of the reactive dye wastewater was 10 and the dye and salt concentrations were 10 g/l and 38.2 g/l, respectively. To determine the dye removal efficiency, the dye concentration was measured before and after filtration. The dye removal efficiency was determined by (1):

$$\textit{Dye removal efficiency}\ (\%) = \frac{C_0 - C}{C_0} \times 100 \qquad (1)$$

where C is the dye concentration after filtration and C_0 is the dye concentration before filtration.

III. Results and Discussion

A. Characterization of PAN/βCD Nanofibers

The solution properties and the morphological results of PAN/βCD and PAN nanofibers are given in Table I. The SEM images and diameter distribution diagrams of nanofibers are shown in Fig. 3.

Bead-free PAN/βCD nanofibers, at the PAN concentration of 13 wt% and with the addition of 10 wt% and 50 wt% βCD, were yielded.

According to Table I, by increasing βCD concentration, the viscosity of the solution was increased and thus the nanofiber diameter was increased.

To prove the presence of βCD within the PAN/βCD nanofibers, chemical analysis was performed using FTIR. The FTIR spectra of pure βCD, PAN and PAN/βCD nanofibers are shown in Fig. 4. βCD had characteristic absorption bands at around 1030, 1080 and 1158 cm^{-1}, corresponding to the coupled C-C and C-O stretching vibrations and asymmetric stretching vibration of C-O-C glycosidic bridge [20].

TABLE I
Solution Properties, Electrospinning Conditions and the Diameters of PAN/βCD and PAN Nanofibers

Sample	Flow rate (ml/h)	Voltage (kV)	βCD concentration (%)	Diameter (nm)	Viscosity (cp)
PAN	0.4	15	0	242.6 ± 39.1	1200
PAN/βCD10	0.4	15	10	322.3 ±39.5	1243
PAN/βCD50	0.4	8.5	50	607.1 ± 100	2605

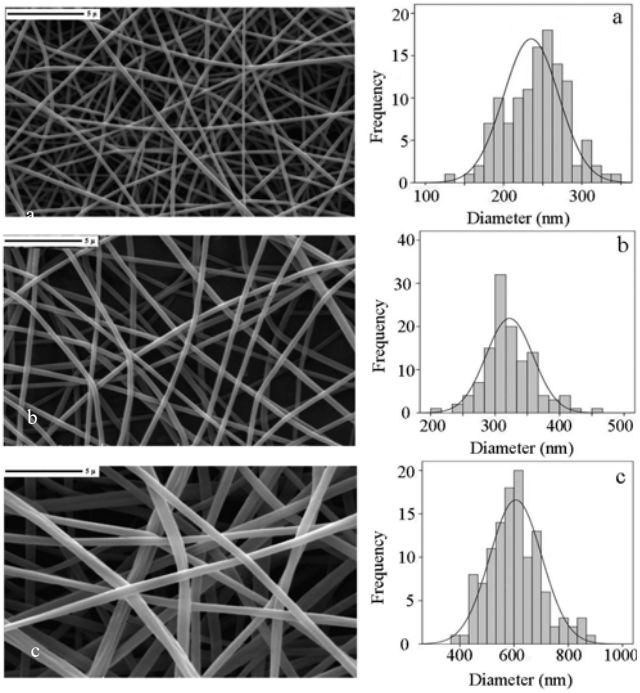

Fig. 3. SEM images and diameter distribution diagrams of (a) PAN, (b) PAN/βCD10 and (c) PAN/βCD50 nanofibers.

According to Fig. 4(a), the characteristic absorption bands of βCD were salient points in the FTIR spectra of PAN/βCD nanofibers, thereby confirming that βCD molecules had been successfully incorporated in the PAN nanofibers.

It should be noted that the presence of βCD molecules on the nanofiber surface is an important property for increasing filtration efficiency by forming inclusion complexes. During the electrospinning process, it is quite possible that some βCD molecules place on the surface of the nanofibers due to phase separation [10]. To confirm the presence of βCD molecules on the surface of fibers, an ATR - FTIR analysis was carried out. Based on the results shown in Fig. 5, the existence of adsorption bands at around 1030, 1080 and 1158 cm^{-1} confirmed that βCD molecules were present on the surface of the nanofibers. This result indicates that the surface of nanofibers was functionalized with βCD. Because of the cavity of βCD molecules, these nanofibers could be used as molecular

filters to remove the organic molecules from the environment.

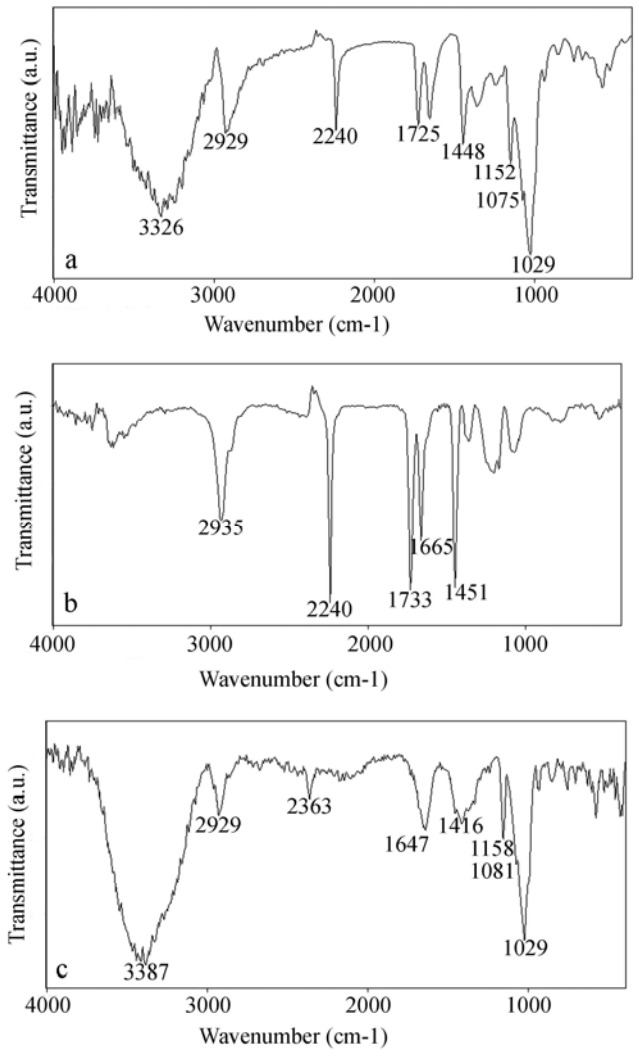

Fig. 4. FTIR spectra of (a) PAN/βCD50 nanofibers, (b) PAN nanofibers and (c) βCD.

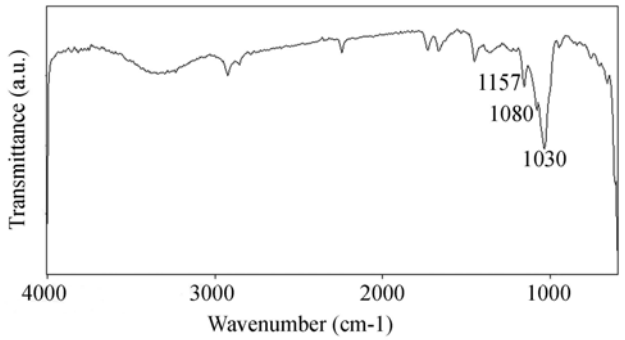

Fig. 5. ATR–FTIR spectrum of PAN/βCD50 nanofibers.

βCDs are known to be crystalline, with two major crystal structures named as "cage" and "channel" types [25]. In the cage structure, the cavity of each molecule is blocked by the neighboring molecules and in the channel type CD, molecules are aligned and stacked on the top of each other, forming long cylindrical channels. This arrangement is formed when the CD molecule forms the inclusion complex with a guest molecule or a polymer chain [25]. The βCD cage crystal has well-known characteristic diffraction peaks at 2θ ~ 10.5°, 12.5°, 19.5° and 21° and the channel structure has two major peaks at around 2θ ~ 11.5° and 18° [11,12]. The XRD pattern of the PAN/βCD nanofibers is shown in Fig. 6. The pattern of PAN/βCD nanofibers illustrated a broad pattern without any strong diffraction peaks. The lack of the peaks of the channel type in PAN/βCD samples confirmed that the inclusion complex between the βCD cavity and the PAN molecular chain had not been formed. Additionally, it was possible that CD molecules were separated from the PAN matrix during electrospinning, forming cage crystal aggregates. But, there were not any peaks related to cage crystals in the XRD pattern, thereby indicating CDs were distributed homogenously in the PAN matrix without forming any crystalline structure. So, their cavities were not blocked, thereby being available to form an inclusion complex with the pollutant molecules in the environment.

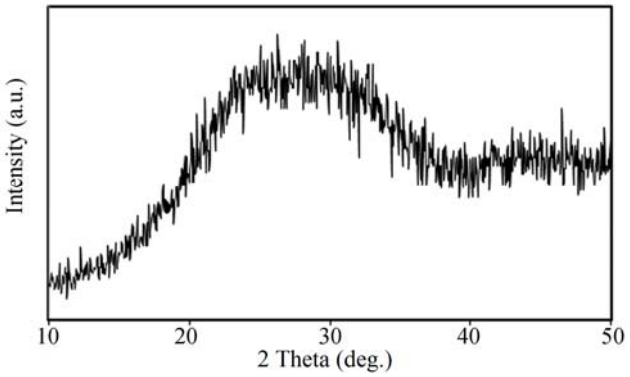

Fig. 6. XRD pattern of PAN/βCD nanofibers.

B. Performance of PAN/βCD Nanofibrous Filters

The results showed that the dye removal efficiency of PAN and PAN/βCD nanofiber mats was 15.5% and 24%, respectively. Although the functionalized nanofiber mats had 54.8% more dye removal efficiency than the non-functionalized nanofiber mats, due to forming an inclusion complex between βCD cavity and dye molecules, the efficiency of PAN/βCD mats was still low. ATR–FTIR spectra of the PAN/βCD nanofiber surface, after the filtration of distilled water for 1 hour, are shown in Fig. 7. The results showed that the βCD peaks at 1030, 1080 and 1158 cm^{-1} were absent after filtration. This showed that βCD was dissolved in water during the filtration process because of the water solubility of βCD molecules (1.85 g/100 ml at 25°C).

Uyar *et al* [10] proved that the combination of CD and nanofibers could improve the efficiency of filters. They used CD functionalized polystyrene nanofibers to trap phenolphthalein (php) molecules from a php solution. They were able to show that PS/βCD electrospun fibers removed php molecules by inclusion complexation with surface associated βCD molecules. Therefore, they recommended using these functionalized nanofibers as

molecular filters and/or nanofilters for filtration/purification/separation purposes. But they disregarded the point that their test condition was static and the filtration operations are mostly dynamic.

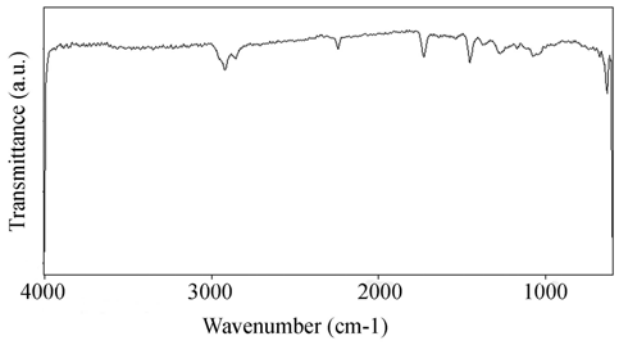

Fig. 7. ATR–FTIR spectrum of PAN/βCD50 nanofibers after filtration.

In our research, it was proved that the PAN/βCD nanofiber mat was not suitable for filtration in a dynamic system and aqueous solution, because the βCD molecules on the surface could be easily removed by water at the applied pressure.

C. β – Cyclodextrin Polymer (βCDP) Production

Cyclodextrins can become water insoluble in two essential ways. The first way refers to the polymerization of βCDs by the reaction between the hydroxyl groups of the molecules with a coupling agent to form oligomers and long-chain polymers, insoluble crosslinked gels, soluble polymers and copolymers. The second way relies on the covalent bonding of βCD molecules to a pre-existing insoluble matrix, like organic and polymeric resins or mineral beads, via several spacer arms [26].

It is known that the mechanism of adsorption on these adsorbents involves several kinds of interactions: physical adsorption in the polymer network, hydrogen bonding between the functional groups of the pollutant and the hydroxyl groups of βCD, and the formation of an inclusion complex due to the βCD molecules through host–guest interactions [27,28].

In this work, we polymerized βCD with citric acid monohydrate as the crosslink agent and polyethylene glycol as modifier, according to the study of Zhao *et al* [29]. After production, β –cyclodextrin polymer (βCDP) was ball milled to form a fine powder, and a particle size of about 397.24 nm was obtained.

The FTIR spectra of the βCDP sample synthesized in our laboratory is given in Fig. 8. According to Fig. 8, an intensive absorption band appeared at 1736 cm^{-1}, which was absent in the βCD spectrum (Fig. 4(c)). This peak was due to the C-O stretching vibration of ester groups and carboxyl groups in βCDP. The peak at 1200 cm^{-1} in Fig. 8 owing to the C–O–C stretching vibration of the ester groups was also absent in the βCD spectrum. The absorption bands of ester groups indicated that some hydroxyl groups of βCD had reacted with the carboxyl groups of citric acid and therefore, a three-dimensional network was formed. Because of the crosslinked network, the βCDP was insoluble in water [29]. The strong and broad bands at 3400 cm^{-1}corresponded to the O–H stretching vibration of the hydroxyl groups in βCD and βCDP. The peak at 2929 cm^{-1} in Fig. 8 corresponded to the CH_2 asymmetric stretching vibration. The C–OH stretching vibration at 1030 cm^{-1}, the C–O–C stretching vibration at 1159 cm^{-1}, and the other absorption bands including 1414 cm^{-1}, 947 cm^{-1}, 858 cm^{-1}, 756 cm^{-1} and 579 cm^{-1} for βCD also appeared nearly at the same wave numbers for βCDP. It could be inferred that the structure characteristics of βCD molecules were well maintained in βCDP [30].

The XRD pattern of βCDP is shown in Fig. 9. There were not any distinct peaks corresponding to the channel type in βCDP. This confirmed that the inclusion complex between the βCD cavities and citric acid molecules and polyethylene glyclol chains, during polymerization had not been formed. So the CD cavity was available to form an inclusion complex with dye molecules.

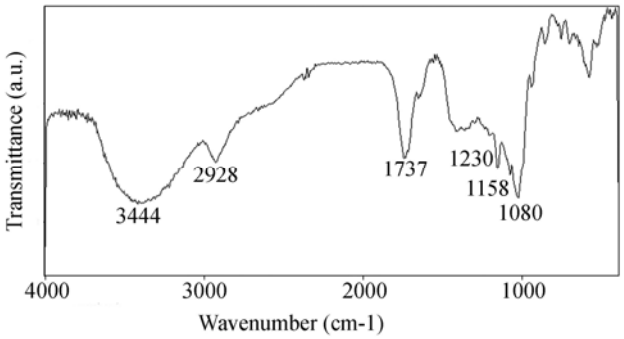

Fig. 8. FTIR spectrum of the synthesized βCDP

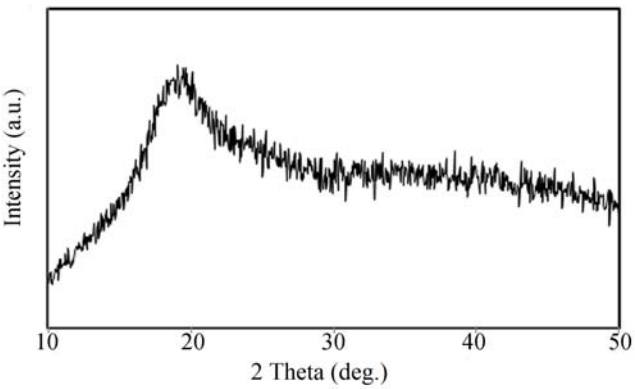

Fig. 9. XRD pattern of βCDP.

D. Characterizations of PAN/βCDP Nanofibers

To study the feasibility of electrospinning βCDP with PAN, the βCDP concentration was chosen to be 15, 25 and 50 wt% with respect to PAN without changing the PAN solution concentration. The electrospinning process was carried out under conditions shown in Table II.

The morphology of electrospun nanofibers is shown in Fig. 10. The surface of nanofibers was relatively uniform with no bead. The solution properties and the

morphological results of PAN/βCDP are given in Table II. According to Table II, the same as with PAN/βCD nanofibers, increasing the βCDP concentration caused an increase in nanofibers diameter due to an increase in the solution viscosity.

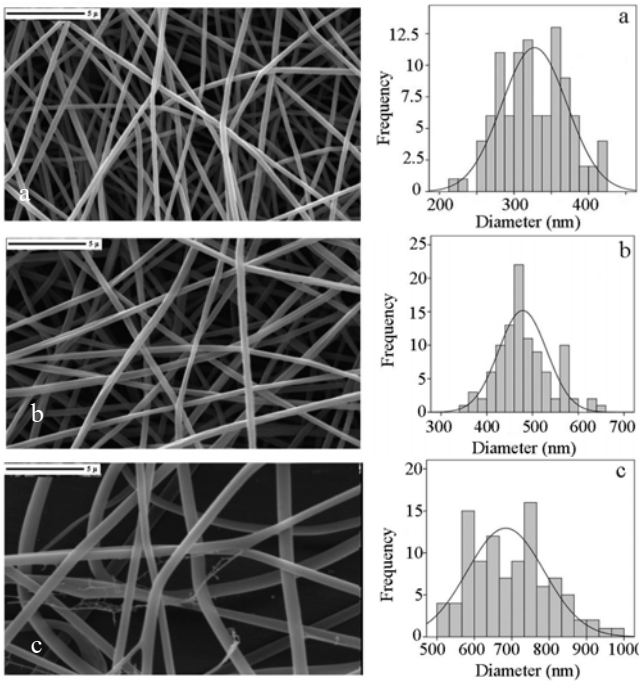

Fig. 10. SEM images and diameter distribution diagrams of (a) PAN/βCDP15, (b) PAN/βCDP25, and (c) PAN/βCDP50 nanofibers.

TABLE II
SOLUTION PROPERTIES AND THE MORPHOLOGICAL RESULTS OF PAN/βCDP AND PAN NANOFIBERS

Solution	Flow rate (ml/h)	Voltage (kV)	βCDP concentration (%)	Nanofiber diameter (nm)	Solution viscosity (cp)
PAN	0.4	15	0	241.0 ± 37.8	1200
PAN/βCDP15	0.4	15	15	327.0 ± 45.3	1872
PAN/βCDP25	0.4	13	25	481.8 ± 59.7	2705
PAN/βCDP50	0.2	8.5	50	697.5± 107.1	-

E. Performance of the Nanofibrous Filter Made by PAN/βCDP Nanofibers

The filtration performance of nanofibrous membranes was investigated using the filtration system mentioned previously. The ATR–FTIR spectra of PAN/βCDP15 nanofiber surface, before and after the filtration of distilled water for 1 hour are shown in Fig. 11. The figure shows that the spectrum did not change after the filtration. The presence of peaks at 1736 and 1250 cm^{-1} in the ATR – FTIR spectrum of PAN/βCDP15 nanofibers after filtration, which are related to the C-O stretching vibration of ester groups and carboxyl groups and the stretching vibration of ester groups in βCDP, shows that βCDP did not dissolve in water during the filtration process.

The dye removal efficiencies of filters, as presented in Table III, showed that the presence of βCDP improved the dye removal efficiency from 15.5% for PAN to 31.4% for PAN/βCDP15 nanofibers. This increase in the efficiency was because of the 3D network of βCDP and the presence of cavities in the βCDP structure, resulting in forming inclusion complexes between the dye molecules and the cavities.

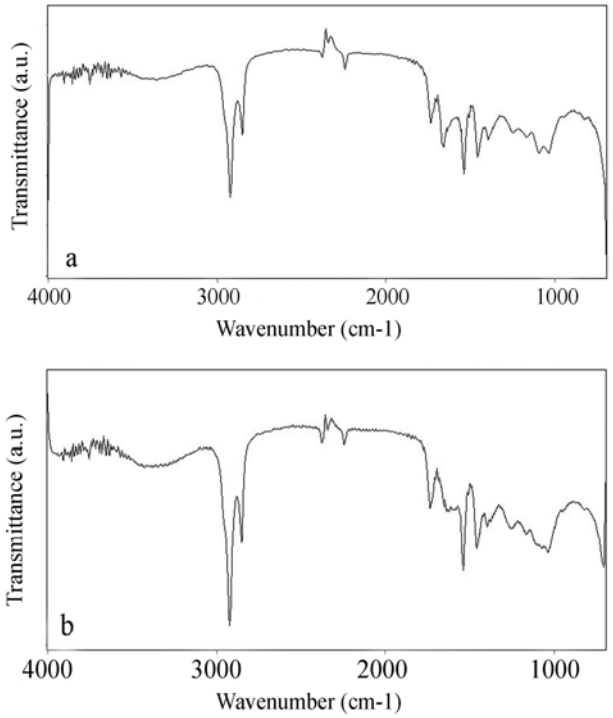

Fig. 11. ATR – FTIR spectra of PAN/βCDP15 nanofibers (a) before and (b) after filtration.

To prove the formation of the inclusion complexes between βCDP cavities and dye molecules, XRD patterns of the filter, before and after filtration, were compared (Fig. 12). In the XRD pattern of the filter before filtration there were no distinct peaks for the channel type, whereas the peaks at 2θ ~ 11.5°, 18° confirmed that an inclusion complex between the βCDP cavities and dye molecules had been formed. However, according to the pattern, the peaks were shifted to right and appeared at 2θ ~ 14° and 25°.

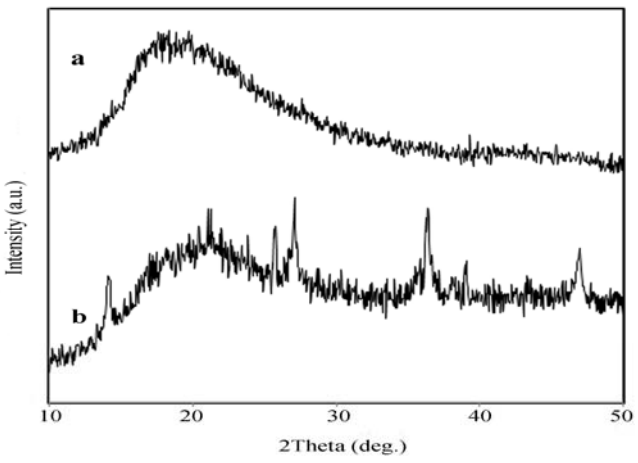

Fig. 12. XRD pattern of PAN/βCDP nanofiber filters (a) before and (b) after filtration.

To increase the dye removal efficiency, different concentrations of βCDP were used and different filters were provided. The results of filtration efficiency in the presence of 15, 25 and 50 wt% βCDP are given in Table III.

TABLE III
THE EFFECT OF βCDP CONCENTRATION ON DYE REMOVAL EFFICIENCY

sample	Nanofiber diameter (nm)	Dye removal efficiency (%)
PAN	241.0 ± 37.8	15.5
PAN/βCDP15	327.0 ± 45.3	31.4
PAN/βCDP25	481.8 ± 59.7	12.1
PAN/βCDP50	697.5 ± 107.1	5.6

Based on the results, the dye removal efficiency was reduced with increasing the βCDP concentration in the polymer solution. When the βCDP concentration was 15wt%, the efficiency was 31.4%, but when the βCDP concentration was increased to 25 and 50 wt%, the dye removal efficiency was decreased to 12.1% and 5.6%, respectively.

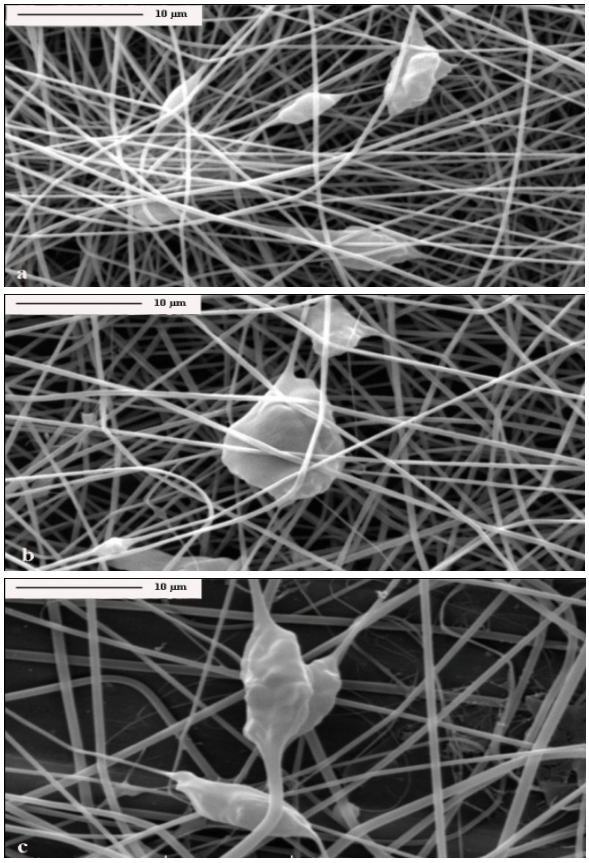

Fig. 13. SEM images of (a) PAN/βCDP15, (b) PAN/βCDP25, (c) PAN/βCDP50 nanofibers.

To identify the reason, the SEM images of nanofiber webs were studied. The SEM images of the webs with different concentrations of βCDP are shown in Fig. 13. According to this figure, there were some βCDP aggregates which caused an increase in the pore size of the web. Also, the results of air permeability tests supported the results obtained by SEM images. The air permeability of webs is shown in Fig. 14. It was shown that with increasing βCDP content, because of βCDP aggregation and the increase in the porosity and the pore size of nanofiber webs, the air permeability of the webs was increased. Although the βCDP can improve the dye removal efficiency, further work should be done to reduce βCDP aggregates and ensure a good dispersion of them in nanofibers. Also, changing the electrospinning conditions such as increasing the temperature or using a co-solvent may cause the βCDP molecules to come on the surface of the nanofibers and absorb more dye molecules by forming more inclusion complexes with them [10].

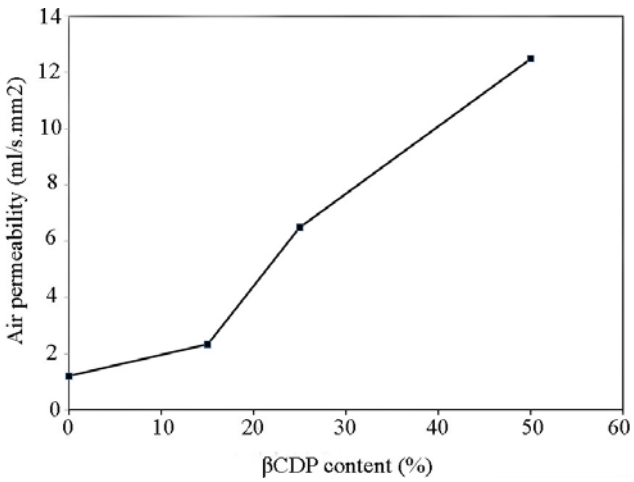

Fig. 14. Air permeability of PAN/βCDP nanofiber webs.

IV. CONCLUSION

In this work, we successfully blended βCD with PAN and electrospun the polymer solution. The subsequent nanofibrous membranes were used to treat the reactive dye wastewater by taking the advantage of the βCD property to form inclusion complexes with guest molecules. It was proved that these functionalized nanofibers could not be used in aqueous solutions in dynamic filtration for removing dye, due to water solubility of βCD. So, we produced βCDP to reduce the water solubility of βCD. The electrospinning process was done using different concentrations of βCDP. In the filtration process, it was found that the dye removal efficiency of βCDP functionalized nanofibrous membranes was about two times more than that of the non functionalized membranes. X- ray diffraction pattern of webs also showed that increasing the efficiency was due to the formation of inclusion complexes between βCDP cavities and dye molecules. Although the goal was fulfilled; there is an opportunity for further work to increase this efficiency. Using co-solvents or changing electrospinning conditions may be required to further place βCDP on the fiber surface and capture more dye molecules by forming inclusion complexes.

REFERENCES

[1] T. Robinson, G. McMullan, R. Marchant and P. Nigam, "Remediation of dyes in textile effluent: a critical review on current treatment technologies with a proposed alternative", *Bioresource Technol.,* vol. 77, pp. 247-255, 2001.

[2] N.F. Ali and R.S.R. EI-Mohamedy, "Microbial decolourization of textile waste water", *J. Saudi Chem. Soc.*, vol 16, pp. 117-123, 2012.

[3] K. Santhy and P. Selvapathy, "Removal of reactive dyes from wastewater by adsorption on coir pith activated carbon", *Bioresource Technol.,* vol. 97, pp. 1329-1336, 2006.

[4] W.J. Lau and A.F. Ismail, "Polymeric nanofiltration membranes for textile dye wastewater treatment: Preparation, performance evaluation, transport modelling, and fouling control - a review", *Desalination,* vol. 245, pp. 321-348, 2009.

[5] E. Forgacs, T. Cserháti and G. Oros, "Removal of synthetic dyes from wastewaters: a review", *Environ. Int.,* vol. 30, pp. 953-971, 2004.

[6] A. Geethakarthi and B. R. Phanikumar, "Industrial sludge based adsorbents/ industrial byproducts in the removal of reactive dyes – A review", *Int. J. Water Resour. Environ. Eng.,* vol. 3, no.1, pp. 1-9, 2011.

[7] I. Petrinic´, N.P.R. Andersen, S. Sostar-Turk and A.M. Le Marechal, "The removal of reactive dye printing compounds using nanofiltration", *Dyes Pigments*, vol. 74, pp. 512-518, 2007.

[8] R. Gopal, S. Kaur, Z. Ma, C. Chan, S. Ramakrishna and T. Matsuura, "Electrospun nanofibrous filtration membrane", *J. Membrane Sci.,* vol. 281, pp. 581–586, 2006.

[9] R. S. Barhate and S. Ramakrishna, "Nanofibrous filtering media: Filtration problems and solutions from tiny materials", *J. Membrane Sci.*, vol. 296, pp.1-8, 2007.

[10] T. Uyar, R. Havelund, Y. Nur, J. Hacaloglu, F. Besenbacher and P. Kingshott, "Molecular filters based on cyclodextrin functionalized electrospun fibers", *J. Membrane Sci.*, vol. 332, pp. 129-137, 2009.

[11] T. Uyar, Y. Nur, J. Hacaloglu and F. Besenbacher, "Electrospinning of functional poly(methyl methacrylate) nanofibers containing cyclodextrin-menthol inclusion complexes ", *Nanotechnology,* vol. 20, pp. 1-10, 2009.

[12] T. Uyar, A. Balan, L. Toppare and F. Besenbacher, "Electrospinning of cyclodextrin functionalized poly(methyl methacrylate) (PMMA) nanofibers", *Polymer,* vol. 50, pp. 475-480, 2009.

[13] L. Li and Y.L. Hsieh "Ultra-fine polyelectrolyte fibers from electrospinning of poly(acrylic acid) ", *Polymer,* vol. 46, pp. 5133–5139, 2005.

[14] R. Ramaseshnan, S. Sundarrajan, Y. Liu, R.S. Barhate, N.L. Lala and S. Ramakrishna, "Functionalized polymer nanofibre membranes for protection from chemical warfare stimulants" *Nanotechnology*, vol. 17, pp. 2947–2953, 2006.

[15] S. Kaur, M. Kotaki, Z. Ma, R. Gopal and S. Ramakrishna, "Oligosaccharide Functionalized Nanofibrous Membrane", *Int. J. Nanosci.,* vol. 5, pp. 1-11, 2006.

[16] J. Bai, Q. Yang, M. Li, Ch. Zhang and L. Yiaoxian, "Synthesis of poly (*N*-vinylpyrrolidone)/_-cyclodextrin composite nanofibers using electrospinning techniques", *J. mater. process. tech.*, vol. 208, pp. 251–254, 2008.

[17] J. Bai, Q. Yang, M. Li, Sh.Wang, Ch. Zhang, Y. Li, "Preparation of composite nanofibers containing gold nanoparticles by using poly(*N*-vinylpyrrolidone) and β- cyclodextrin", *Mater. Chem. Phys.*, vol. 111, pp. 205–208, 2008.

[18] T. Uyar, P. Kingshott and F. Besenbacher, "Electrospinning of Cyclodextrin–Pseudopolyrotaxane Nanofibers", *Angew. Chem. Int. Ed.*, vol. 47, pp. 9108 –9111, 2008.

[19] T. Uyar and F. Besenbacher, "Electrospinning of cyclodextrin functionalized polyethylene oxide (PEO) nanofibers", *Eur. Polym. J.,* vol. 45, pp. 1032-1037, 2009.

[20] T. Uyar, R. Havelund, J. Hacaloglu, X. Zhou1, F. Besenbacher and P. Kingshott, "The formation and characterization of cyclodextrin functionalized polystyrene nanofibers produced by electrospinning", *Nanotechnology*, vol. 20 pp. 1-14, 2009.

[21] T. Uyar, J. Hacaloglu, F. Besenbacher, "Electrospun polystyrene fibers containing high temperature stable volatile fragrance/flavor facilitated by cyclodextrin inclusion complexes", *React. Funct. Polym., vol.* 69, pp. 145–150, 2009.

[22] T. Uyar, R. Havelund, Y. Nur, A. Balan, J. Hacaloglu, L. Toppare, F. Besenbacher and P. Kingshott, "Cyclodextrin functionalized poly(methyl methacrylate) (PMMA) electrospun nanofibers for organic vapors waste treatment", *J. Membrane Sci.*, vol. 365, pp. 409–417, 2010.

[23] W. Zhang, M. Chen and G. Diao, "Electrospinning β-cyclodextrin/poly (vinyl alcohol) nanofibrous membrane for molecular capture", *Carbohyd. Polym.,* vol. 86, pp. 1410– 1416, 2011.

[24] F. Basiri, S. A. Hosseini Ravandi, M. Feiz and A. Moheb, "Recycling of Direct Dyes Wastewater by Nylon-6 Nanofibrous Membrane", *Curr. Nanosci.*, vol. 7, pp**.** 633-639, 2011.

[25] P. J. ,Brown and K. Stevens, "*Nanofibers and Nanotechnology in Textiles*", 1st ed., Ch. 11, A. E. Tonelli, The Textile Institute and Woodhead publishing, Cambridge, UK: 2007, pp. 299-316.

[26] G. Crini and M. Morcellet, "Synthesis and applications of adsorbents containing cyclodextrins", *J. Sep. Sci,* vol. 25, pp. 789-813, 2002.

[27] G. Crini,,"Studies on adsorption of dyes on beta-cyclodextrin polymer", *Bioresource Technol.,* vol. 90, pp. 193-198, 2003.

[28] É. Fenyvesi and K. Balogh, "CD-containing sorbents for removal of toxic contaminants from waste water", *Cyclodextrin News*, vol. 23, no. 4, 2009.

[29] D. Zhao, L. Zhao, C. Zhu, Z. Tian and X. Shen, "Synthesis and properties of water-insoluble [beta]-cyclodextrin polymer crosslinked by citric acid with PEG-400 as modifier", *Carbohyd. Polym.,* Vol. 78, pp. 125-130, 2009.

[30] D. Zhao, L. Zhao, Ch. Sh. Zhu, W. Q. Huang and J. L. Hu, "Water-insoluble *b*-cyclodextrin polymer crosslinked by citric acid: synthesis and adsorption properties toward phenol and methylene blue", *J. Incl. Phenom. Macrocycl. Chem.*, vol. 63, pp. 195–201, 2009.